

## RESEARCH ARTICLE

# Meteorological conditions during periods of low wind speed and insolation in Germany: The role of weather regimes

Fabian Mockert<sup>1</sup>  | Christian M. Grams<sup>1</sup>  | Tom Brown<sup>2,3</sup> | Fabian Neumann<sup>2,3</sup>

<sup>1</sup>Department Troposphere Research, Institute of Meteorology and Climate Research (IMK-TRO), Karlsruhe Institute of Technology (KIT), Karlsruhe, Germany

<sup>2</sup>Department of Digital Transformation in Energy Systems, Institute of Energy Technology, Technische Universität Berlin, Berlin, Germany

<sup>3</sup>Energy System Integration (ESI), Institute for Automation and Applied Informatics (IAI), Karlsruhe Institute of Technology (KIT), Karlsruhe, Germany

## Correspondence

Fabian Mockert, Department Troposphere Research, Institute of Meteorology and Climate Research (IMK-TRO), Karlsruhe Institute of Technology (KIT), PO 3640, 76021 Karlsruhe, Germany.  
 Email: [fabian.mockert@kit.edu](mailto:fabian.mockert@kit.edu)

## Funding information

Helmholtz Association, Grant/Award Numbers: VH-NG-1243, VH-NG-1352; KIT Center for Mathematics in Sciences, Engineering, Economics; KIT Young Investigator Network (YIN) Grant 2019; Deutsche Forschungsgemeinschaft, Grant/Award Number: SFB/TRR 165

## Abstract

Renewable power generation from wind and solar energy is strongly dependent on the weather. To plan future sustainable energy systems that are robust to weather variability, a better understanding of why and when periods of low wind and solar power output occur is valuable. We call such periods of low wind speed and insolation “Dunkelflauten”, the German word for “dark wind lulls”. In this article, we analyse the meteorological conditions during Dunkelflauten in Germany by applying the concept of weather regimes. Weather regimes are quasi-stationary, recurrent and persistent large-scale circulation patterns that explain multi-day atmospheric variability (5–15 days). We use a regime definition that allows us to distinguish four different types of blocked regimes, characterized by high-pressure situations in the North Atlantic-European region. We find that Dunkelflauten in Germany occur mainly in winter when the solar power output is low due to the seasonal cycle of solar irradiance and wind power output drops for several consecutive days. A high-pressure system over Germany, associated with the European Blocking regime, is responsible for most of the Dunkelflauten. Dunkelflauten during the Greenland Blocking regime are associated with colder temperatures than usual, causing higher electricity demand, and would present a particular challenge as space heating becomes electrified in the future. Furthermore, we show that Dunkelflauten occur predominantly when a weather regime is well established and persists longer than usual. Our study provides novel insight into the occurrence and meteorological characteristics of Dunkelflauten, which is essential for planning resilient energy systems and supporting grid operators to prepare for potential shortages in supply.

## KEYWORDS

Dunkelflauten, energy demand, predictability, renewable energies, subseasonal prediction, weather regimes

This is an open access article under the terms of the [Creative Commons Attribution-NonCommercial](https://creativecommons.org/licenses/by-nc/4.0/) License, which permits use, distribution and reproduction in any medium, provided the original work is properly cited and is not used for commercial purposes.

© 2023 The Authors. *Meteorological Applications* published by John Wiley & Sons Ltd on behalf of Royal Meteorological Society.

## 1 | INTRODUCTION

One of the main objectives of the European Green Deal is to achieve climate neutrality for all countries in the European Union by 2050, in line with the Paris Agreement to limit global temperature increases to well below 2°C (European Commission, 2019). A key strategy to achieve climate neutrality is to raise the share of wind and solar power in Europe's electricity supply, and then to shift as much of the energy demand as possible to electricity. Wide-ranging electrification of all sectors would lead to a drastic increase in electricity consumption in Germany by 2045 (TSO, 2022). Depending on the scenario, German transmission system operators (TSOs) expect the gross electricity consumption to double by 2045 compared to 2020. To serve this demand, the TSOs project the installed capacities of onshore wind, offshore wind and solar photovoltaics (PV) in Germany to rise from 116 GW in 2020 up to 616 GW in 2045 (TSO, 2022).

With the increase in the share of variable renewable generation in the power system and the increase in electricity demand due to electrification (Bloomfield, Brayshaw, Troccoli, et al., 2021; Edenhofer et al., 2011), the power system becomes increasingly sensitive to meteorological conditions (Bloomfield et al., 2016; van der Wiel et al., 2019a). Consequently, there is a rising need for balancing the spatial and temporal variability of renewable power output to guarantee stable electricity supply. Seasonal variability can be balanced locally by the co-deployment of wind and solar technologies (Heide et al., 2010; Pozo-Vázquez et al., 2004; Santos-Alamillos et al., 2015). Daily variations of solar power can be balanced by storage or through flexibility from demand side management by the likes of battery-powered electric vehicles (Brown et al., 2018). Power to gas units and long-term thermal energy storage were shown to support balancing large-scale and seasonal variations of electricity supply and demand. Some of these technologies can also be used to manage variability in power outputs over several days up to weeks. However, unlike for seasonal storage where the balancing needs are predictable, the operation on these multi-day time scales requires more detailed knowledge of the imminent meteorological conditions. Therefore, meteorological variability on a multi-day to week time range must be considered when planning a reliable energy system with a high share of renewable technologies (Grams et al., 2017).

Meteorological conditions of multi-day events with low power output by renewable technologies can strain the energy system. In the following, we refer to these periods of low solar and wind feed-in as “Dunkelflauten”, from the German word for “dark wind lulls”.

Dunkelflauten have been the subject of numerous studies under different names: low-energy production and energy shortfall events (van der Wiel et al., 2019a, 2019b), low production events (Drücke et al., 2021; Kaspar et al., 2019), peak demand and peak demand-net-renewables events (Bloomfield, Suitters, & Drew, 2020) and energy compound events (Otero et al., 2022). While van der Wiel et al. (2019a), Bloomfield, Suitters, and Drew (2020) and Otero et al. (2022) take the demand side into account, Kaspar et al. (2019) and Drücke et al. (2021) base their definition of Dunkelflauten exclusively on the availability of renewables.

Several studies, such as Drücke et al. (2021) for Germany and van der Wiel et al. (2019a) for Europe, suggest that a high-pressure system in Central Europe is responsible for these low production events. The large-scale meteorological conditions in the North Atlantic-European region during such events can be described by weather regimes. Weather regimes are quasi-stationary, persistent and recurrent large-scale flow patterns in the mid-latitudes (Michelangeli et al., 1995; Vautard, 1990). Weather regimes modulate surface weather in continent-size regions and on multi-day to weekly time scales (Büeler et al., 2021). Thereby, weather regimes cause substantial multi-day variability in the European energy sector (van der Wiel et al., 2019b; Zubiate et al., 2017), in particular wind power (Grams et al., 2017).

To forecast Dunkelflauten events, or more generally the energy supply, grid-point-based forecast methods or indirect pattern-based methods have been suggested (cf. Bloomfield, Brayshaw, Gonzalez, & Charlton-Perez, 2021; Soret et al., 2019). A grid-point forecast uses grid-point surface meteorological forecasts (e.g., 10-m wind) to estimate a relevant power quantity (e.g., national wind power output). In a pattern-based forecast of the same power quantity, the large-scale atmospheric flow is first assigned to a pre-identified circulation pattern and, in a second step, the surface impact is estimated. Bloomfield, Brayshaw, Gonzalez, and Charlton-Perez (2021) compare two pattern-based methods, namely the previously mentioned weather regime approach and an approach based on energy system data rather than large-scale meteorological fields, called targeted circulation types (Bloomfield, Suitters, & Drew, 2020). Bloomfield, Brayshaw, Gonzalez, and Charlton-Perez (2021) show that grid-point forecasts have higher skill at short lead times (days 0–10) than pattern-based methods. At extended lead times (day 12+), pattern-based methods can show greater skill than the grid-point forecasts. Weather regime forecasts show higher skill in week 3 (days 19–25) than targeted circulation types for Central and Northern European countries, likely because of their physical grounding (Faranda et al., 2016, 2017; Hochman et al., 2021). Forecasts on the time scale of 10–30 days, also

referred to as subseasonal to seasonal (S2S) forecasting range, become increasingly important for the energy sector, as they fill the gap between weather forecasts and monthly or seasonal outlooks (White et al., 2017, 2022). In our analysis, we, therefore, link Dunkelflauten to weather regimes.

Blocking conditions are prone to cause below-average power output by wind and solar PV in Central Europe (Grams et al., 2017; van der Wiel et al., 2019b). The negative North Atlantic Oscillation (NAO) phase is associated with cold and weak wind conditions (Bloomfield, Suiters, & Drew, 2020; Tedesco et al., 2022; van der Wiel et al., 2019b). However, not every blocking condition or negative NAO phase leads to Dunkelflauten in Germany. To accurately forecast Dunkelflauten events, more information about the weather regimes that lead to Dunkelflauten is necessary.

In the present study, we aim to shed light on the meteorological conditions under which Dunkelflauten in Germany occur and how they are linked to the occurrence of weather regimes. Furthermore, we aim to understand how regimes related to Dunkelflauten differ from those not associated with a Dunkelflaute.

This rest of the article is structured as follows. Data and methods are described in Section 2. In Section 3, we describe the statistical characteristics of Dunkelflauten in Germany, discuss the meteorological conditions during Dunkelflauten and analyse the relationship between capacity factor, temperature and electricity demand anomalies during Dunkelflauten. Conclusions from this study and potential use cases of the presented results are highlighted in Section 4.

## 2 | DATA AND METHODS

### 2.1 | Reanalysis

Reanalysis data from the European Centre for Medium-Range Weather Forecasts (ERA5) for 1979–2018 form the basis for this study (Hersbach et al., 2020). The reanalyses serve as input data to compute the weather regimes (500-hPa geopotential height), to generate composites of atmospheric field variables during Dunkelflauten (100-m wind speed, surface net solar radiation and surface net solar radiation for clear skies, 2-m temperature, sea-level pressure) and to calculate the capacity factors (100-m wind speed, surface roughness, direct, diffuse and top of the atmosphere influx, albedo). We use ERA5 interpolated from its native reduced-Gaussian grid to a regular lat.–long. grid with 0.5° grid spacing and a temporal resolution of 3 h for calculating the weather regimes (see Section 2.2) and meteorological composites. We use the original grid spacing of 0.25° and hourly resolution to

compute the capacity factors and Dunkelflauten with the *atlite* library (see Sections 2.3 and 2.4).

### 2.2 | Weather regimes

To identify the large-scale atmospheric circulation during Dunkelflauten events, we use the definition of 7-year-round weather regimes by Grams et al. (2017). Regimes are identified based on an empirical orthogonal function analysis of 10-day low-pass-filtered geopotential height anomalies at 500 hPa (Z500, 3-hourly) and a k-means clustering in the North Atlantic-European region (30°–90° N, 80° W–40° E). Individual weather regime life cycles are identified using the projection of the instantaneous Z500 anomalous field onto the cluster mean. The projection is normalised by the standard deviation over the 1979–2019 period to yield a weather regime index (IWR) for each of the seven regimes, following Michel and Rivière (2011). During an active weather regime, the IWR is above 1.0 for at least 5 days and includes the maximum of all IWRs. The onset of the regime is defined as the first time step of  $IWR > 1.0$  (cf. Büeler et al., 2021; Grams et al., 2017). Time steps not attributed to a regime life cycle are labelled as “no regime”.

The seven weather regimes can be separated into three cyclonic regimes, namely Atlantic Trough (AT), Zonal Regime (ZO) and Scandinavian Trough (ScTr). These cyclonic regimes are characterised by low-pressure systems in the North Atlantic-European region. Additionally, there are four blocked regimes, namely the Atlantic Ridge (AR), European Blocking (EuBL), Scandinavian Blocking (ScBL) and Greenland Blocking (GL), which are dominated by high-pressure systems.

### 2.3 | Capacity factors

Our study focuses on the power output by renewable energy sources, namely solar as well as onshore and offshore wind power in Germany. As a measure for the power output, we use the resources' capacity factor time series, which denotes the ratio between the actual power output and the rated capacity.

The capacity factors are computed with the Python library *atlite*, which converts weather data (e.g., wind speed and solar influx) into energy system data (e.g., capacity factors) (Hofmann et al., 2021). To generate the capacity factor, *atlite* uses the ERA5 reanalysis dataset at 0.25° grid spacing and 1-hourly temporal resolution. For the wind capacity factor calculation, *atlite* uses the 100-m wind speed and the surface roughness as input data. For calculating the solar capacity factor, the direct,

diffuse and top-of-the-atmosphere influx and the albedo are needed as input data.

Atlite assumes the geographic distribution of installed wind and solar capacities to be proportional to the technology's capacity factors (i.e., more wind farms in windy areas, see Figure S1). We use a solar panel model based on Huld et al. (2010) with a solar azimuth of 180° (South) and a slope of 35°. As a reference onshore wind turbine, we use the Vestas V112 3-MW model and for offshore the 5-MW NREL Reference Turbine.

Based on a linear regression between simulated and historical capacity factor time series, the capacity factors are corrected to match the observed time series (OPSD, 2020) more closely (Figure S2). The total power output by renewable energy sources is expressed by combining the three different capacity factor time series to one combined capacity factor by applying a weighted mean with currently installed capacities per technology as weights. For Germany in 2018, these are as follows: 44% solar (45.9 GW), 50% onshore wind (53.0 GW) and 6% offshore wind (6.4 GW) (IRENA, 2019).

The optimised approach of the geographic distribution of installed wind and solar capacities will likely lead to a too high estimate of the capacity factors, but it is less dependent on political decision-making. The effect of the too-high capacity factor is damped by scaling the capacity factors with the historical capacity factor time series of Germany given by OPSD (2020).

For Germany, the individual capacity factors of wind and solar have a pronounced seasonal cycle (Figure 1). On average, the onshore and offshore wind capacity factors are lower in summer than in winter, and the solar capacity factor is higher in summer than in winter. By

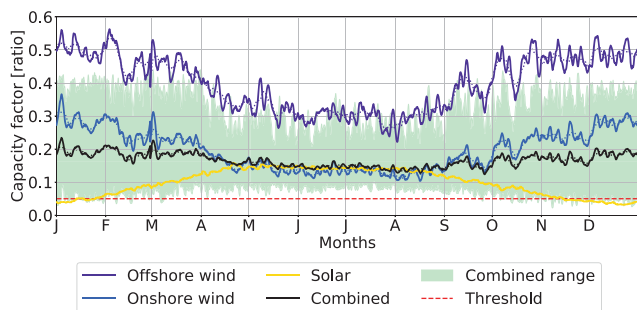


**FIGURE 1** Average seasonal cycle of the capacity factors in Germany for 1979–2018 (based on hourly time steps, 48-h running mean [solid lines] and weekly running mean [dotted lines]). The combination of onshore wind (blue), offshore wind (purple) and solar (yellow) capacity factors, weighted on the installed capacity, is represented by the combined capacity factor (black). The range (minimum, maximum) of the 48-h running mean combined capacity factor throughout the 40 year (1979–2018) period is shown (mint green shading). The red horizontal line marks a threshold of 0.06.

combining the capacity factors of wind and solar, weighted by the installed capacity, the mean seasonal variation is balanced.

From here on, we refer to the combined capacity factor when writing the capacity factor unless otherwise stated.

## 2.4 | Dunkelflauten

We are interested in periods when little or no energy is available by wind and solar power for at least 2 days. In this study, we define Dunkelflauten as periods with 48-h running mean capacity factors below a threshold of 0.06. We have defined the 48-h threshold according to the study of Kaspar et al. (2019) and because energy storage is more problematic for periods with low renewable feed-in longer than 2 days (Schmidt et al., 2019). The frequency and duration of Dunkelflauten events can be controlled by modifying the threshold value. Here, we set the threshold at 0.06 to obtain a similar number of Dunkelflauten per year as shown by Kaspar et al. (2019) (three to four Dunkelflauten per year with a threshold of 0.1). Our results regarding the central time of occurrence and meteorological characteristics of Dunkelflauten hold under modification of the threshold value (e.g., 0.05 or 0.10), although we detect fewer and shorter events for smaller thresholds and more and longer events for higher thresholds.

All time steps contributing to a running mean below the threshold are considered part of the Dunkelflaute. Therefore, the minimum duration of a Dunkelflaute is 48 h.

We categorise Dunkelflauten according to the dominant weather regime in this period. In case several weather regimes contribute the same number of hours to a Dunkelflaute, the Dunkelflaute is associated with the weather regime that occurs at the onset of the Dunkelflaute since this is the weather regime that triggers the Dunkelflaute in the first place. With this definition, there are eight categories of Dunkelflauten: Dunkelflauten related to one of the seven weather regimes or to the “no regime”.

As will be shown later (Figure 2), Dunkelflauten occur mainly in winter. To capture the sequence of challenging renewable supply conditions, we consider years centred on winter, starting in July and ending in June of the following year. For simplicity, we refer to these periods as extended winter.

## 2.5 | Electricity demand

To investigate weather-induced variability in electricity demand, we also incorporate daily mean electricity demand

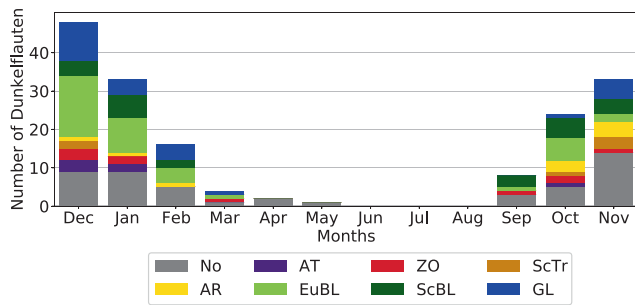


**FIGURE 2** Monthly distribution of Dunkelflauten with the dominant weather regimes of Dunkelflauten indicated by the colour of the bars. The amount of Dunkelflauten is measured on an absolute scale for the 40-year period from 1979 to 2018. AT, Atlantic Trough; ZO, Zonal Regime; ScTr, Scandinavian Trough; AR, Atlantic Ridge; EuBL, European Blocking; ScBL, Scandinavian Blocking; GL, Greenland Blocking.

data from Bloomfield, Brayshaw, and Charlton-Perez (2020) into our analysis. The model builds on 2-m temperature data from the ERA5 reanalysis and uses a multiple-linear regression model for 28 European countries from 1979 to 2018. The model focuses on weather-dependent parameters, and therefore neglects human behavioural factors (day-of-week and long-term socio-economic trends). The demand time series we use can be interpreted as the demand that would have been expected on each weather day in 1979–2018, with no day-of-week effects and the prevailing socio-economic conditions of 2017. This data reflects the temperature dependence of the electricity demand in 2017. We use the daily demand time series to compute the average daily demand anomalies during Dunkelflauten, compared to daily climatology. Owing to electrification in the space heating sector in Germany (BDEW, 2022), it can be expected that the electricity demand will become more temperature-dependent in future scenarios, so results with the historical demand model are likely to underestimate the significance of the weather-dependent demand. Data is limited to daily weather-dependent demand, excluding the diurnal cycle of demand (Bloomfield, Brayshaw, & Charlton-Perez, 2020).

### 3 | RESULTS

This section first gives a general overview of Dunkelflauten in Germany and their link to weather regimes (Section 3.1). Subsequently, differences in the origin of Dunkelflauten are revealed by analysing composites of different atmospheric field variables (Section 3.2). In Section 3.3, we investigate whether weather regime life cycles associated with Dunkelflauten differ from general regime life cycle characteristics. In Section 3.4 we

consider the electricity demand model of Bloomfield, Suijters, and Drew (2020) to relate our results from Section 3.2 to the electricity demand during Dunkelflauten events.

#### 3.1 | Characteristic of Dunkelflauten in Germany

By our definition, a Dunkelflaute is a rare event indicating a period of low combined wind and solar power output. In the 40-year period from 1979 to 2018, we detected 169 Dunkelflauten, which cumulates to an average of 4 Dunkelflauten per year. These Dunkelflauten have a pronounced seasonal cycle (Figure 2), with the bulk of Dunkelflauten in autumn (September to November) and winter (December to February) and none in summer (June to August). The seasonality of Dunkelflauten is explainable by the seasonal cycle of the capacity factors (Figure 1).

The distribution width of the combined capacity factor, using the 48-h running mean in the 40-year period, is the smallest in summer, and the minimum value of the summer distribution (0.064) is above the Dunkelflauten threshold. In the winter half-year, the combined capacity factor distribution varies over a larger range, occasionally reaching values below the Dunkelflauten threshold. Values below the threshold are due to the combination of low 48-h running mean solar capacity factors (average of 0.053 in winter time) and occasional drops in the wind capacity factors below the threshold. In winter, solar power cannot always compensate for the occasional lack of wind power. In summer, the solar capacity factor (average of 0.139) is well above the Dunkelflauten threshold and can thus compensate for periods of low wind capacity factors.

The frequency of Dunkelflauten varies not only throughout the year but also inter-annually. On average, 4.3 Dunkelflauten occur per year (Figure S3). Most Dunkelflauten per extended winter period have occurred in 1995/1996 and 1996/1997, with 9 and 10 Dunkelflauten, respectively. The median duration of a Dunkelflaute is 3.2 days (77.5 h) with a maximum duration of 8 days (Figure S4). Only 15 Dunkelflauten events (9%) exceed the duration of 5 days, which is the minimum duration of weather regimes. No Dunkelflaute reaches the mean duration of weather regimes, which is 11.3 days. The shortest possible duration of a Dunkelflaute is 2 days by definition. The duration of Dunkelflauten has a similar seasonal cycle as the amount of Dunkelflauten, with the longest Dunkelflauten in December. Figure S5 provides a detailed visualisation of all Dunkelflauten over the years.

With the help of weather regimes for the Northern Atlantic-European region, we can describe and forecast

large-scale circulation and wind and solar irradiation patterns. The frequency distribution of weather regimes during Dunkelflauten differs from its climatological distribution (Figure 3).

The year-round climatological frequency distribution of weather regimes is well balanced throughout cyclonic (Atlantic Trough, Zonal Regime, Scandinavian Trough) and blocked weather regimes (Atlantic Ridge, European Blocking, Scandinavian Blocking, Greenland Blocking) with frequencies between 9.2% and 11.0% (Figure 3a, top row). However, for Dunkelflauten periods, the distribution of the weather regimes is not in balance (Figure 3b, top row). Dunkelflauten occur predominantly in three of the four blocked weather regimes, European, Scandinavian and Greenland Blocking, among which Dunkelflauten occur most frequently during European Blocking (22.2%). As Dunkelflauten mainly occur in autumn and winter (Figure 2), we compare the frequency distributions for these seasons separately (Figure 3a,b, second and third row). The preference of Dunkelflauten occurrence during the three blocked weather regimes over the cyclonic weather regimes remains, but differences in the preferred frequency of blocked regimes occur. In autumn, Scandinavian Blocking is 7% more frequent during Dunkelflauten compared to all autumn days (12.6% vs. 19.7%, Figure 3). In winter, the frequency of European and Greenland Blocking is increased by 19% and 6% (an increase from 9.8% up to 28.6% and from 10.9% up to 17.3%, respectively, Figure 3) during Dunkelflauten compared to the overall frequency in winter. Thus, Dunkelflauten preferentially occur during the blocked European, Scandinavian and Greenland Blocking regimes.

### 3.2 | Meteorological parameters during Dunkelflauten

To further shed light on the meteorological conditions during Dunkelflauten and to estimate the severity of Dunkelflauten during different regimes in terms of surface weather, we analyse anomaly composites (relative to the 30-day running mean climatology) of different atmospheric field variables (100-m wind speed, solar irradiation, 2-m temperature, sea-level pressure) in the North Atlantic-European region. The solar irradiation is given as the ratio of the daily sums of the surface net solar radiation (SSR in ERA5 reanalysis) and the surface net solar radiation for clear skies (SSRC in ERA5 reanalysis). This quantity reflects the fraction of the maximum possible daily insolation (cf. Grams et al., 2017).

The composites of all Dunkelflauten events (Figure 4a–c) represent the mean atmospheric conditions. Low wind speeds are associated with weak surface pressure gradients. Weak pressure gradients can occur in the centre of a high-pressure system or the saddle point between multiple high- and low-pressure systems. On average, weak pressure gradients in the centre and northwestern edge of a surface anticyclone over Europe cause low wind speeds during Dunkelflauten in Germany (Figure 4a). Insolation is only marginally altered in comparison to the 30-day running mean climatology (Figure 4b). This suggests that Dunkelflauten are primarily due to a lack of wind power. On average, 2-m temperature anomalies of up to 2 K occur in Central Europe (Figure 4c).

Analysing Dunkelflauten separated by weather regimes demonstrates that the conditions for Dunkelflauten can be achieved by different atmospheric conditions

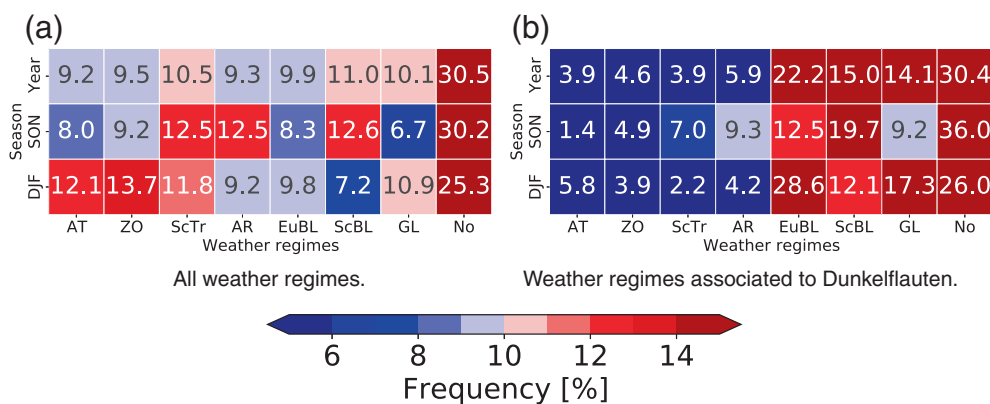


**FIGURE 3** Weather regime frequencies for all weather regimes (a) and all weather regimes associated with a Dunkelflaute (b). Shown for all seasons of the year combined, only autumn (SON: September–November) and only winter (DJF: December–February). Data for the years 1979–2018. AT, Atlantic Trough; ZO, Zonal Regime; ScTr, Scandinavian Trough; AR, Atlantic Ridge; EuBL, European Blocking; ScBL, Scandinavian Blocking; GL, Greenland Blocking.

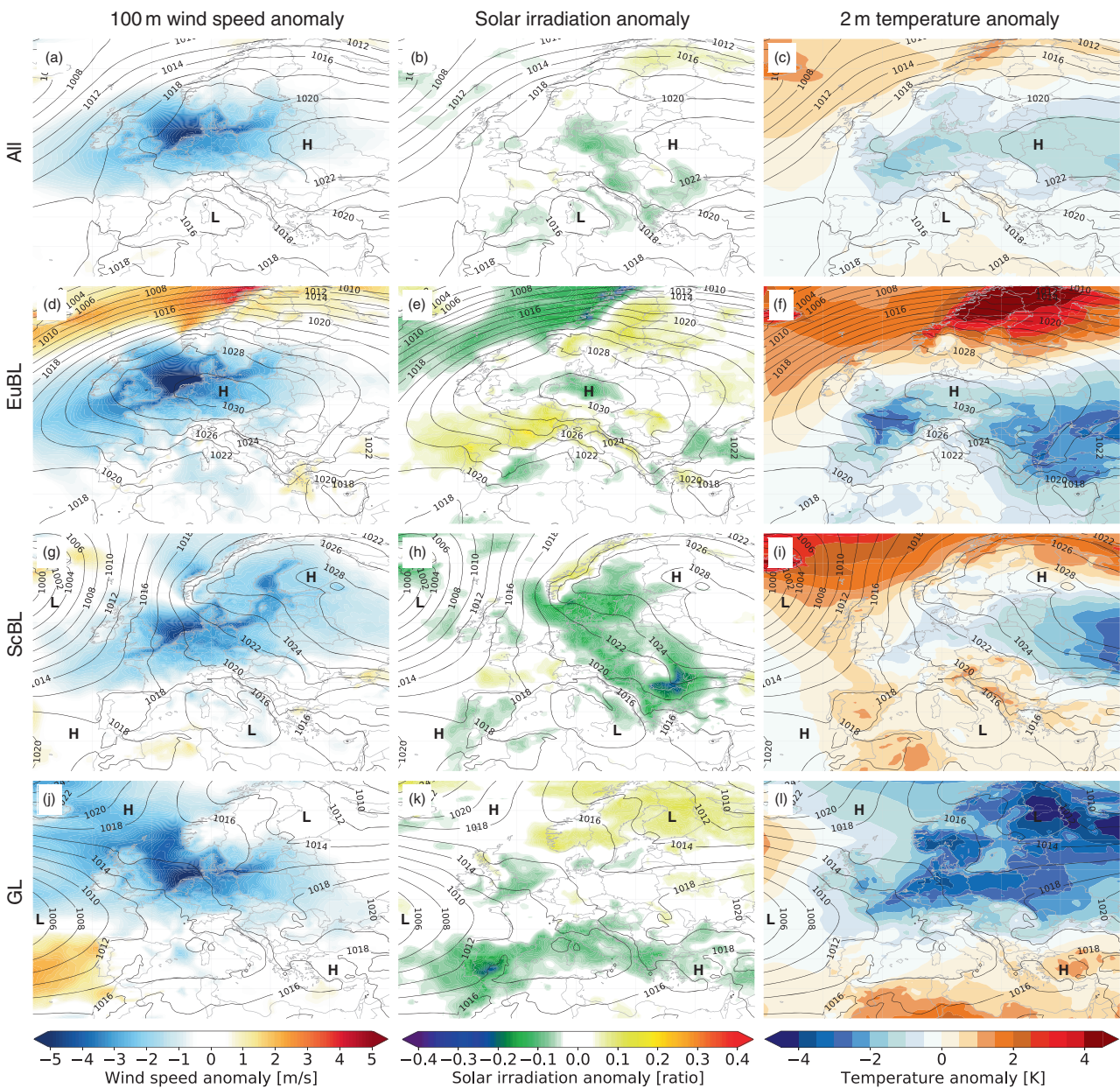


**FIGURE 4** Composites of atmospheric field variables for different types of Dunkelflauten. The rows show all Dunkelflauten events (a–c), European Blocking (EuBL) Dunkelflauten (d–f), Scandinavian Blocking (ScBL) Dunkelflauten (g–i) and Greenland Blocking (GL) Dunkelflauten (j–l). The first column shows 100-m wind speed anomalies (with respect to a 30-day running mean climatology) as shading, the second column the anomaly in the daily fraction of maximum solar insolation (with respect to the 30-day running mean climatology) and the third column 2-m temperature anomalies (with respect to the 30-day running mean climatology). Each composite shows the absolute sea-level pressure with a 2-hPa contour interval.

(Figure 4d–l). Thus, the mean conditions for all events do not reflect variability in meteorological conditions during Dunkelflauten events imposed by different weather regimes.

The three dominant Dunkelflauten types, classified by weather regimes as European, Scandinavian and Greenland Blocking (shown in Figure 3), all indicate low wind speeds in the North Sea region due to weak pressure gradients, but the pressure system patterns differ

between the Dunkelflauten types (Figure 4d,g,j). For the three dominant Dunkelflauten types, there are only weak modulations of irradiation (Figure 4e,h,k). Strong differences in the temperature anomalies among these Dunkelflauten types exist (Figure 4f,i,l).

During European Blocking Dunkelflauten, low wind speeds in northern Germany and the North Sea region occur in the centre of a high-pressure system centred over Germany (Figure 4d).

In contrast, low wind speeds for Scandinavian and Greenland Blocking Dunkelflauten occur in a region of weak pressure gradients due to a quadrupole of two high- and two low-pressure systems centred over Germany. For Scandinavian Blocking Dunkelflauten (Figure 4g), the low pressure dominates near Iceland and in the Mediterranean, and high pressure prevails in the vicinity of the Azores and Scandinavia. The quadrupole is reversed for Greenland Blocking Dunkelflauten (Figure 4j). Low-pressure centres are located over the Atlantic north of the Azores and Scandinavia, and high pressure extends over the Icelandic region and southeastern Europe.

Solar irradiation is only marginally altered for the different Dunkelflauten types. Minor positive (negative) anomalies occur in the south (north) of Germany during European Blocking Dunkelflauten (Figure 4e). For Scandinavian Blocking Dunkelflauten, only a negative solar irradiation anomaly is detected in northern Germany (Figure 4h), and no solar irradiation anomalies are present in Germany during Greenland Blocking Dunkelflauten (Figure 4k).

For European Blocking Dunkelflauten, the 2-m temperature, in particular in Germany but also in Western and Eastern Europe in general, is up to 2 K below the 30-day running mean climatology (Figure 4f). For Scandinavian Blocking Dunkelflauten, the south of Germany experiences marginally warmer and the north of Germany marginally colder 2-m temperatures in comparison to climatology (Figure 4i). During Greenland Blocking Dunkelflauten, Germany is under the influence of substantial negative 2-m temperature anomalies, which are up to 4 K colder compared to the 30-day running mean climatology (Figure 4l). The negative 2-m temperature anomaly is present in Western, Central, Eastern, and Northern Europe, as well as in Russia.

Analysing the temperature anomalies in more detail for Greenland Blocking Dunkelflauten shows that the negative anomalies in Germany and Northern Europe are already present 6 days prior to the onset of the Dunkelflauten (Figure S6). Cold polar air is advected to Europe prior to the onset of the Dunkelflaute. Subsequently, the cold air mass becomes stationary in Germany and even endures the Dunkelflaute itself. The long-lasting negative temperature anomalies amplify the potential stress that an energy system faces during and after Dunkelflauten related to Greenland Blocking.

In summary, exploring the meteorological conditions during Dunkelflauten related to different weather regimes unveiled that not all Dunkelflauten are caused by high pressure over Germany and go along with cold conditions. For Dunkelflauten related to Greenland Blocking, Germany is located in a saddle point between weather systems. Importantly, Greenland Blocking

Dunkelflauten are cold Dunkelflauten, causing unusually cold conditions for a prolonged period, and, therefore, likely stress the energy system.

### 3.3 | Characteristics of weather regimes associated to Dunkelflauten

The strong link of Dunkelflauten to specific weather regimes raises the question of whether regime life cycles associated with Dunkelflauten differ from the general characteristics of such cycles. Therefore, we now explore life cycle characteristics such as the regime duration and the relation of Dunkelflauten occurrence and regime onset and decay.

First, we investigate the duration of weather regimes with Dunkelflauten. To account for the small sample size of weather regimes, such as 52 Greenland Blocking life cycles in the months from November to March (NDJFM) over the years 1979–2018, a direct comparison of average life cycle durations is not suitable. Instead, we employ a bootstrapping method following the approach by Wernli and Papritz (2018) and explained in detail in Section 2.5 of Büeler et al. (2020): For each weather regime category, we create two bootstrapped distributions, one for the Dunkelflauten and one as a climatological reference. Each distribution consists of 1000 random samples with the same number of elements as the number of Dunkelflauten for the respective weather regime category. The elements for the Dunkelflauten samples are drawn from all Dunkelflauten events with replacements. The elements for a sample of the climatological reference distribution are drawn with replacements from all regime life cycles in the 40-year period. To retain the seasonal cycle of Dunkelflauten in the random climatological samples, we draw for each Dunkelflaute event a corresponding random element in a  $\pm 45$ -day window around the same day of the year but for a random year. For each of the 1000 random samples, we then calculate the mean life cycle duration to obtain a distribution of the mean life cycle duration for Dunkelflauten and in the climatological reference.

Following Wernli and Papritz (2018) and Büeler et al. (2020), we test whether the life cycle duration for Dunkelflauten is statistically significantly longer on a 20% level if the 20% percentile of the Dunkelflauten distribution is greater than the 80% percentile of the reference distribution (indicated as orange triangles in Figure 5). The rather high significance level of 20% is chosen to account for the relatively high number of life cycles with a Dunkelflaute compared to those without a Dunkelflaute in extended winter. For instance, of the 52 Greenland Blocking life cycles in November to March

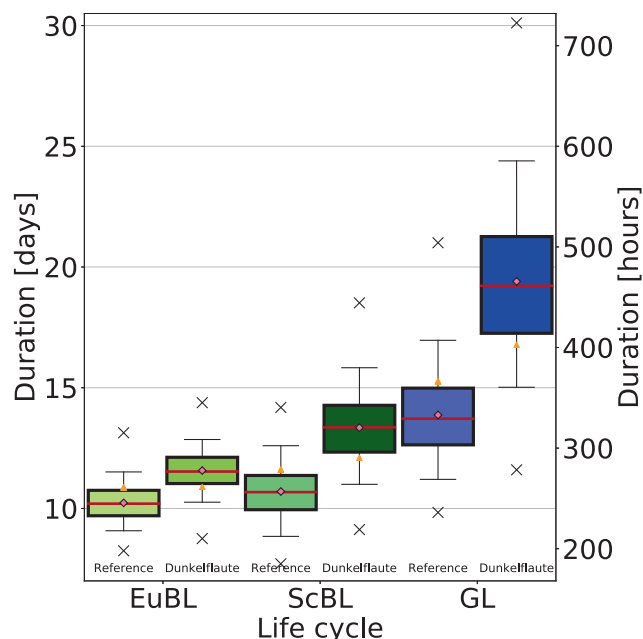


**FIGURE 5** Bootstrapped distribution of mean regime life cycle duration associated with Dunkelflauten. Climatological distribution (pale coloured bar plots left) and life cycles associated with Dunkelflauten (dark coloured bar plots right) for European Blocking (EuBL, light green), Scandinavian Blocking (ScBL, dark green) and Greenland Blocking (GL, blue). Pink diamonds represent the mean, red horizontal lines the median, boxes the 25%–75% percentile, whiskers the 5%–95% percentiles and outliers the minimum and maximum values. Orange triangles indicate the 80% and 20% percentiles for the climatological and Dunkelflauten distribution, respectively.

(NDJFM), 18 feature a Dunkelflaute, roughly a share of 1/3. Drawing the climatological reference samples only from those life cycles not featuring a Dunkelflaute would yield similar results as reported below, but on a 10% significance level (not shown).

The reference samples' mean life cycle duration distribution reveals differences between the European, Scandinavian and Greenland Blocking weather regimes (Figure 5, left columns). Whereas European and Scandinavian Blocking weather regime life cycles are active for 10.2 and 10.7 days, respectively, Greenland Blocking life cycles have a mean lifespan of 13.8 days.

Comparing the Dunkelflauten distribution (Figure 5, right columns) to the reference distribution (Figure 5, left columns) for each weather regime separately shows significantly longer life cycle durations for the Dunkelflauten samples. Life cycles associated with European and Scandinavian Blocking Dunkelflauten have a mean duration of 11.6 and 13.3 days, respectively (an increase in duration of 14% and 24% compared to the reference samples). For life cycles associated with Greenland Blocking Dunkelflauten, the difference is even more

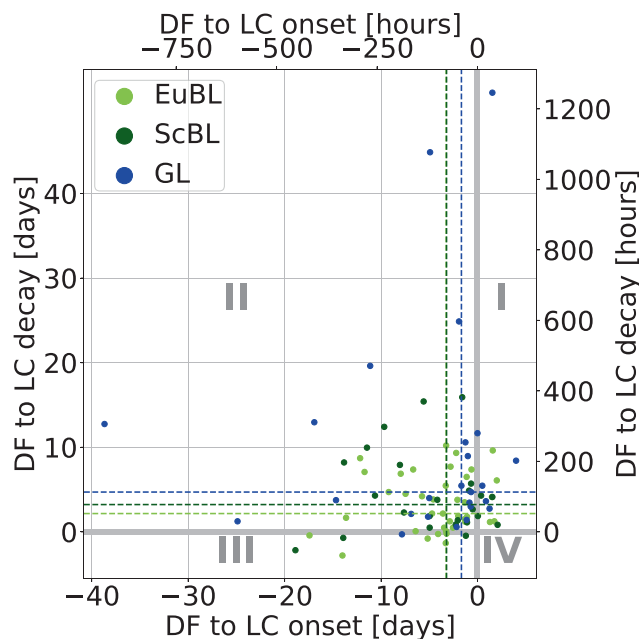


**FIGURE 6** Onset and decay of Dunkelflauten (DF) in relation to the onset and decay of the associated regime life cycle (LC) for European (EuBL), Scandinavian (ScBL) and Greenland Blocking (GL) Dunkelflauten. The median time differences between the onsets and decays for each Dunkelflauten category are represented by the dashed vertical and horizontal lines, respectively. The four quadrants distinguish the following categories: I. A Dunkelflaute sets in before the life cycle and decays during the active life cycle; II. A Dunkelflaute sets in during the associated life cycle and decays during the active life cycle; III. A Dunkelflaute sets in during an active life cycle and decays after the decay of the life cycle; IV. A Dunkelflaute sets in prior to the onset of the life cycle and lasts longer than the life cycle; therefore decays after the decay of the life cycle.

pronounced with an average life cycle duration of 19.4 days (an increase of 41%). All three life cycle duration differences are significant at the 20% level.

The results of this bootstrapping method indicate that Dunkelflauten occur in longer-lived life cycles compared to life cycles in the same seasonal period.

Considering the average life cycle duration of 11–20 days and the Dunkelflauten duration of 3–9 days, the subsequent question is whether Dunkelflauten occur at specific times of the associated life cycle.

Dunkelflauten are mostly fully embedded in the regime life cycle associated with the Dunkelflaute (Figure 6 quadrant II, indicating that the Dunkelflauten onset is after the life cycle onset and the Dunkelflauten decay is prior to the life cycle decay). In numbers, this translates to an average (median) onset of Dunkelflauten of 3.3/3.2/1.7 days after the onset of the life cycle and an average decay of 2.2/3.2/4.7 days prior to the decay of the life cycle for European/Scandinavian/Greenland Blocking, respectively.

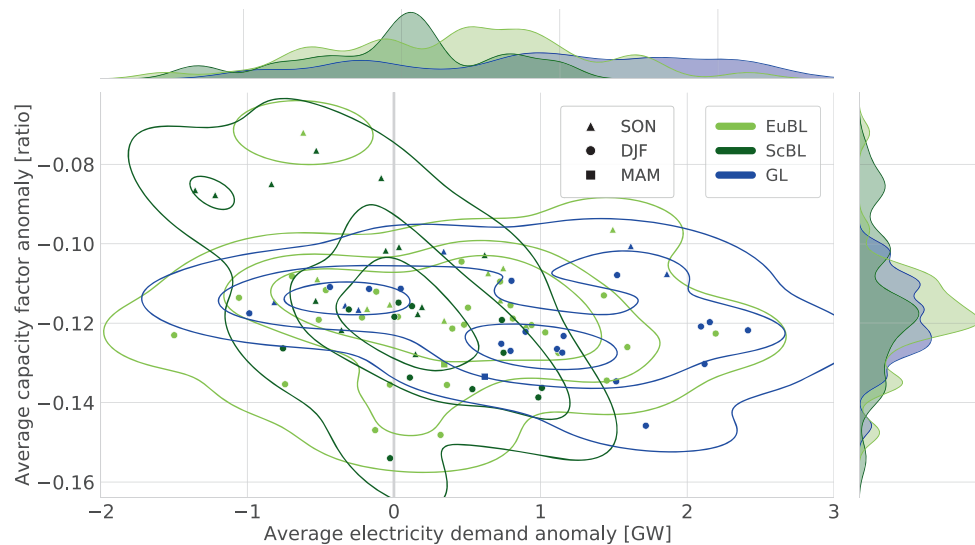


**FIGURE 7** Average capacity factor and electricity demand anomalies during different Dunkelflauten types in Germany. The electricity demand is based on the prevailing socioeconomic conditions of 2017. All European, Scandinavian, and Greenland Blocking Dunkelflauten are represented with their regime colour. The shape of the marker indicates the season of each Dunkelflaute. The 2D density distribution of each Dunkelflaute type is given as shading in the main figure and as 1D distribution in the two marginal figures. EuBL, European Blocking; ScBL, Scandinavian Blocking; GL, Greenland Blocking.

Thus, Dunkelflauten occur mainly in the well-developed and stable phases of regime life cycles.

### 3.4 | Electricity demand during Dunkelflauten

With negative 2-m temperature anomalies during European and Greenland Blocking Dunkelflauten (shown in Section 3.2), we expect a higher heating demand in Germany due to colder than normal temperatures in wintertime. The combination of a Dunkelflaute event with low renewable power output and an increased electricity demand due to cold temperatures will likely put stress on the energy system.

The capacity factors during the three dominant Dunkelflauten types are reduced on average from 0.18 to 0.06 (Figure 7, right marginal figure), which is a relative reduction of 66% compared to winter climatology.

Whereas there is no anomalously high average electricity demand for Scandinavian Blocking Dunkelflauten (Figure 7, top marginal figure), the average electricity demand during Dunkelflauten is marginally increased for European Blocking Dunkelflauten (average increase of 0.5 GW) and more strongly increased for Greenland Blocking Dunkelflauten (average increase of 1.0 GW, but values also reaching up to 3.2 GW). Absolute values of the electricity demand in the period from November to March range from 44.5 GW up to 76.5 GW. Therefore, during Dunkelflauten, the electricity demand may rise by

up to 7%, using the socio-economic conditions of 2017. Although we did not directly investigate the dependence of electricity demand on 2-m temperature, the latter is likely a main meteorological driver of demand (Bloomfield, Suitters, & Drew, 2020) (Figure 7). Also, as shown in Section 3.2, marked temperature anomalies occur in Germany during Dunkelflauten. In particular, persistent low temperatures accompany the low power output during the cold Greenland Blocking Dunkelflaute (Figures 4I and S6). Thus we conclude that Greenland Blocking Dunkelflauten are likely the most challenging periods for the operation of an energy system with a high share of renewables.

An even larger increase in electricity demand can be expected in the future due to the transition to a fully renewable energy system, so this problem gets amplified.

## 4 | DISCUSSION AND CONCLUSIONS

The present study links large-scale atmospheric circulation patterns, called weather regimes, and periods with low wind and solar power in Germany called Dunkelflauten. Following Kaspar et al. (2019), Dunkelflauten are defined as periods with a low combined capacity factor of solar photovoltaics, onshore wind and offshore wind in Germany, lasting for at least 2 days, using the atlite energy system model framework and meteorological data from ERA5 reanalysis. We then link each Dunkelflaute

event from 1979 to 2018 to one of the 7-year-round weather regimes or the “no regime” (Grams et al., 2017).

Dunkelflauten are mainly found in Germany during autumn and winter. This seasonal effect is due to the low mean solar capacity factor in winter. Thus Dunkelflauten are primarily caused by low wind speed conditions.

Differentiating Dunkelflauten by the prevalent large-scale atmospheric flow, using weather regimes, helps us to identify different atmospheric patterns leading to Dunkelflauten in Germany. Three blocking weather regimes are most frequently associated with Dunkelflauten: European Blocking with 22% of all Dunkelflauten, Scandinavian Blocking with 15% and Greenland Blocking with 14%. A high-pressure system over Germany and Central Europe is the most frequent Dunkelflauten pattern and is associated with the European Blocking weather regime.

The meteorological conditions during Greenland, Scandinavian and European Blocking Dunkelflauten differ: A high-pressure system extends over Central Europe during European Blocking Dunkelflauten, and Germany is located in the centre of the high pressure with prevalent low pressure gradients and consequently low winds. In contrast, during Greenland Blocking and Scandinavian Blocking Dunkelflauten, Central Europe is located in a saddle point of a quadripole of two high- and two low-pressure systems, likewise causing low pressure gradients and low winds in Germany. Thus, it is essential to analyse Dunkelflauten not as one composite but separately between different weather regime patterns. Greenland Blocking Dunkelflauten are considered to be cold Dunkelflauten. These Dunkelflauten periods are up to 4°C colder than the 30-day running climatology, increasing the electricity demand from electrical heating. Increased electricity demand in periods of lower than normal power output by renewable energy sources can put stress on the energy system.

Weather regime life cycles associated with Dunkelflauten also differ in their general characteristics: Life cycles associated with Dunkelflauten are longer-lived than usual, especially for Greenland Blocking weather regimes, with life cycles on average 5 days longer than the November to March (NDJFM) climatology (19 days compared to 14 days). The life cycles of weather regimes begin well before the onset of the Dunkelflauten and end thereafter. Thus, Dunkelflauten occur when weather regime life cycles are well established. This is useful from a forecast perspective, as knowledge about upcoming blocking weather regimes can help prepare the energy system for an imminent supply shortage.

Our results confirm findings from previous studies and extend the knowledge of Dunkelflauten. Kaspar et al. (2019) and Drücke et al. (2021) also found

Dunkelflauten in Germany, mainly in autumn and winter. They categorised Dunkelflauten by Grosswetterlagen (Grosswetterlagen classify the circulation in Europe with 29 different weather types, focusing more on the regional conditions than the continental-scale large-scale weather regimes used here) and identified the “Grosswetterlage GWL9” as the most frequent pattern for Dunkelflauten in Germany. GWL9 has characteristics comparable to those of the European Blocking weather regime. van der Wiel et al. (2019b) identified the NAO-weather regime, derived from the four weather regime classification by Cassou (2008), Michelangeli et al. (1995) and Vautard (1990), and strongly correlating with the Greenland Blocking weather regime, to be the scenario with reduced energy production and increased energy demand for Europe. The increased electricity demand in Greenland Blocking Dunkelflauten, using the electricity demand model of Bloomfield, Suitters, and Drew (2020), is likely to intensify in the future due to Germany's transition to electrical heating. In the past 10 years, the contribution of electrical heating to the heating structure of new buildings has doubled, from 24% in 2012 up to 50% in 2022 (BDEW, 2022). Otero et al. (2022) show the link of energy compound events in Germany, simultaneous episodes of low renewable energy production (wind plus solar power) and high electricity demand, and weather regimes. Energy compound events in Germany are more frequent in European and Greenland Blocking weather regimes. These results are consistent with the cold Dunkelflauten in our research.

We extend the knowledge of Dunkelflauten in Germany by analysing weather regime life cycles and meteorological conditions associated with different Dunkelflauten. Dunkelflauten, especially the cold Greenland Blocking Dunkelflauten, are positioned in the well-established phase of longer-lived weather regime life cycles. Furthermore, Dunkelflauten occur not only when high pressure prevails but also in conditions when Germany is in the middle between pronounced weather systems elsewhere.

Although we find robust results and confirm previous findings, our choices for defining Dunkelflauten (minimum duration, capacity factor threshold) and weather regimes (low-pass filter, minimum duration, life cycle definition) might affect the results. Therefore we stress that the results are valid only for the specific definitions used here. In particular, other regime definitions might identify different weather regimes relevant for Dunkelflauten. Also, our regime definition allows for parallel regime life cycles. However, here we attributed Dunkelflauten based on the highest number of time steps with maximum regime projections during the Dunkelflaute which does not consider the potential simultaneous

projection into another regime. Future avenues of research could explore factors that may contribute to the occurrence of Dunkelflauten besides the already identified long duration of the weather regime and investigate whether Dunkelflauten occur in parallel regime life cycles.

The link of Dunkelflauten to weather regimes provides a forecast opportunity on the subseasonal to seasonal (S2S) range. Bloomfield, Brayshaw, Gonzalez, and Charlton-Perez (2021) showed that pattern-based methods, such as weather regimes, outperform grid-point forecasts for lead times larger than 12 days for the European national power forecasts. Weather regime forecasts can fill the gap between short-range weather prediction and long-range seasonal outlooks for the energy sector (White et al., 2017). With the results of our study, we expect to more accurately forecast Dunkelflauten using weather regimes, as the likelihood of a potential Dunkelflaute could be identified not only by the forecasted weather regime but also by the forecasted duration of a weather regime life cycle.

Based on our results in combination with the results by Büeler et al. (2021), showing the modulation of surface weather by weather regimes and the promising skill of weather regimes on the subseasonal to seasonal range, we see weather regime forecasts as an essential tool for energy system operators to prepare for multi-day supply shortages.

## AUTHOR CONTRIBUTIONS

**Fabian Mockert:** Conceptualization (equal); data curation (lead); formal analysis (lead); methodology (lead); software (lead); visualization (lead); writing – original draft (lead); writing – review and editing (equal). **Christian M. Grams:** Conceptualization (equal); funding acquisition (equal); project administration (equal); supervision (equal); writing – review and editing (equal). **Tom Brown:** Conceptualization (equal); funding acquisition (equal); project administration (equal); supervision (equal); writing – review and editing (equal). **Fabian Neumann:** Conceptualization (equal); data curation (supporting); methodology (supporting); software (supporting); supervision (equal); writing – review and editing (equal).

## ACKNOWLEDGEMENTS

This project was initiated and partially funded through a KIT Young Investigator Network (YIN) Grant 2019. FM further acknowledges from the KIT Center for Mathematics in Sciences, Engineering and Economics under the seed funding programme. The contribution of CMG is funded by the Helmholtz Association as part of the Young Investigator Group “Sub-seasonal Predictability: Understanding the Role of Diabatic Outflow”

(SPREADOUT, grant VH-NG-1243). The research was partially embedded in the subprojects A8 of the Transregional Collaborative Research Center SFB/TRR 165 “Waves to Weather” (<https://www.wavestoweather.de>) funded by the German Research Foundation (DFG). FN and TB gratefully acknowledge funding from the Helmholtz Association under grant VH-NG-1352. We thank Hannah Bloomfield for providing the demand time series and the members of the Energy Meteorology and Dynamical Processes groups at the University of Reading for the fruitful discussions. Open Access funding enabled and organized by Projekt DEAL.

## CONFLICT OF INTEREST STATEMENT

All authors declare that they have no conflicts of interest.

## DATA AVAILABILITY STATEMENT

Code is available on the GitHub repository [https://github.com/fmockert/dunkelflauten\\_DE](https://github.com/fmockert/dunkelflauten_DE). The ERA5 data can be obtained from the Climate Data Store <https://cds.climate.copernicus.eu/#/home>. Weather regime data are available from CMG upon request. The historical power output and in-installed capacities can be retrieved from [https://data.open-power-system-data.org/time\\_series/2019-06-05](https://data.open-power-system-data.org/time_series/2019-06-05). The demand data is available at <https://doi.org/10.17864/1947.273>.

## ORCID

Fabian Mockert  <https://orcid.org/0000-0002-3222-6667>  
 Christian M. Grams  <https://orcid.org/0000-0003-3466-9389>

## REFERENCES

- BDEW. (2022) Entwicklung der Beheizungsstruktur im Wohnungsneubau. Available at: <https://www.bdew.de/service/daten-und-grafiken/entwicklung-beheizungsstruktur-baugenehmigungen/> [Accessed 16th December 2022].
- Bloomfield, H.C., Brayshaw, D. & Charlton-Perez, A. (2020) *Era5 derived time series of european country-aggregate electricity demand, wind power generation and solar power generation*. University of Reading, Reading. Available from: <https://doi.org/10.17864/1947.273>
- Bloomfield, H.C., Brayshaw, D.J., Shaffrey, L.C., Coker, P.J. & Thornton, H.E. (2016) Quantifying the increasing sensitivity of power systems to climate variability. *Environmental Research Letters*, 11, 124025. Available from: <https://doi.org/10.1088/1748-9326/11/12/124025>
- Bloomfield, H.C., Brayshaw, D.J., Troccoli, A., Goodess, C.M., De Felice, M., Dubus, L. et al. (2021) Quantifying the sensitivity of European power systems to energy scenarios and climate change projections. *Renewable Energy*, 164, 1062–1075. Available from: <https://doi.org/10.1016/j.renene.2020.09.125>
- Bloomfield, H.C., Brayshaw, D.J., Gonzalez, P.L.M. & Charlton-Perez, A. (2021) Pattern-based conditioning enhances sub-seasonal prediction skill of European national energy variables.

- Meteorological Applications*, 28, e2018. Available from: <https://doi.org/10.1002/met.2018>
- Bloomfield, H.C., Sutters, C.C. & Drew, D.R. (2020) Meteorological drivers of European power system stress. *Journal of Renewable Energy*, 2020, 1–12. Available from: <https://doi.org/10.1155/2020/5481010>
- Brown, T., Schlachtberger, D., Kies, A., Schramm, S. & Greiner, M. (2018) Synergies of sector coupling and transmission reinforcement in a cost-optimised, highly renewable European energy system. *Energy*, 160, 720–739. Available from: <https://doi.org/10.1016/j.energy.2018.06.222>
- Büeler, D., Beerli, R., Wernli, H. & Grams, C.M. (2020) Stratospheric influence on ecmwf sub-seasonal forecast skill for energy-industry-relevant surface weather in european countries. *Quarterly Journal of the Royal Meteorological Society*, 146, 3675–3694. Available from: <https://doi.org/10.1002/qj.3866>
- Büeler, D., Ferranti, L., Magnusson, L., Quinting, J.F. & Grams, C.M. (2021) Year-round sub-seasonal forecast skill for Atlantic-European weather regimes. *Quarterly Journal of the Royal Meteorological Society*, 147, 4283–4309. Available from: <https://doi.org/10.1002/qj.4178>
- Cassou, C. (2008) Intraseasonal interaction between the Madden-Julian Oscillation and the North Atlantic Oscillation. *Nature*, 455, 523–527. Available from: <https://doi.org/10.1038/nature07286>
- Drücke, J., Borsche, M., James, P., Kaspar, F., Pfeifroth, U., Ahrens, B. et al. (2021) Climatological analysis of solar and wind energy in Germany using the Grosswetterlagen classification. *Renewable Energy*, 164, 1254–1266. Available from: <https://doi.org/10.1016/j.renene.2020.10.102>
- Edenhofer, O., Pichs-Madruga, R., Sokona, Y., Seyboth, K., Arvizu, D. & Bruckner, T. (2011) Summary for policy makers. Available at: <https://orbit.dtu.dk/en/publications/summary-for-policy-makers>. [Accessed 16th December 2022].
- European Commission. (2019) The European Green Deal. Available at: [https://eur-lex.europa.eu/resource.html?uri=cellar:b828d165-1c22-11ea-8c1f-01aa75ed71a1.0002.02/DOC\\_1\&format=PDF](https://eur-lex.europa.eu/resource.html?uri=cellar:b828d165-1c22-11ea-8c1f-01aa75ed71a1.0002.02/DOC_1\&format=PDF) [Accessed 16th December 2022].
- Faranda, D., Masato, G., Moloney, N., Sato, Y., Daviaud, F., Dubrulle, B. et al. (2016) The switching between zonal and blocked mid-latitude atmospheric circulation: a dynamical system perspective. *Climate Dynamics*, 47, 1587–1599. Available from: <https://doi.org/10.1007/s00382-015-2921-6>
- Faranda, D., Messori, G. & Yiou, P. (2017) Dynamical proxies of North Atlantic predictability and extremes. *Scientific Reports*, 7, 41278. Available from: <https://doi.org/10.1038/srep41278>
- Grams, C.M., Beerli, R., Pfenninger, S., Staffell, I. & Wernli, H. (2017) Balancing Europe's wind-power output through spatial deployment informed by weather regimes. *Nature Climate Change*, 7, 557–562. Available from: <https://doi.org/10.1038/NCLIMATE3338>
- Heide, D., von Bremen, L., Greiner, M., Hoffmann, C., Speckmann, M. & Bofinger, S. (2010) Seasonal optimal mix of wind and solar power in a future, highly renewable Europe. *Renewable Energy*, 35, 2483–2489. Available from: <https://doi.org/10.1016/j.renene.2010.03.012>
- Hersbach, H., Bell, B., Berrisford, P., Hirahara, S., Horányi, A., Sabater, J.M. et al. (2020) The ERA5 global reanalysis. *Quarterly Journal of the Royal Meteorological Society*, 146, 1999–2049. Available from: <https://doi.org/10.1002/qj.3803>
- Hochman, A., Messori, G., Quinting, J.F., Pinto, J.G. & Grams, C.M. (2021) Do Atlantic-European weather regimes physically exist? *Geophysical Research Letters*, 48, e2021GL095574. Available from: <https://doi.org/10.1029/2021GL095574>
- Hofmann, F., Hampp, J., Neumann, F., Brown, T. & Hörsch, J. (2021) atlite: a lightweight python package for calculating renewable power potentials and time series. *Journal of Open Source Software*, 6, 3294. Available from: <https://doi.org/10.21105/joss.03294>
- Huld, T., Gottschalg, R., Beyer, H.G. & Topič, M. (2010) Mapping the performance of PV modules, effects of module type and data averaging. *Solar Energy*, 84, 324–338. Available from: <https://doi.org/10.1016/j.solener.2009.12.002>
- IRENA. (2019) *Renewable capacity statistics 2019*. International Renewable Energy Agency (IRENA), Abu Dhabi.
- Kaspar, F., Borsche, M., Pfeifroth, U., Trentmann, J., Drücke, J. & Becker, P. (2019) A climatological assessment of balancing effects and shortfall risks of photovoltaics and wind energy in Germany and Europe. *Advances in Science and Research*, 16, 119–128. Available from: <https://doi.org/10.5194/asr-16-119-2019>
- Michel, C. & Rivière, G. (2011) The link between Rossby wave breakings and weather regime transitions. *Journal of the Atmospheric Sciences*, 68, 1730–1748. Available from: <https://doi.org/10.1175/2011JAS3635.1>
- Michelangeli, P.-A., Vautard, R. & Legras, B. (1995) Weather regimes: recurrence and quasi stationarity. *Journal of Atmospheric Sciences*, 52, 1237–1256. Available from: [https://doi.org/10.1175/1520-0469\(1995\)052%3C1237:WRAQS%3E2.0.CO;2](https://doi.org/10.1175/1520-0469(1995)052%3C1237:WRAQS%3E2.0.CO;2)
- OPSD. (2020) Time series renewable power plants. Available at: [https://data.open-power-system-data.org/time\\_series/2020-10-06](https://data.open-power-system-data.org/time_series/2020-10-06). [Accessed 16th December 2022].
- Otero, N., Martius, O., Allen, S., Bloomfield, H. & Schaeffli, B. (2022) Characterizing renewable energy compound events across Europe using a logistic regression-based approach. *Meteorological Applications*, 29, e2089. Available from: <https://doi.org/10.1002/met.2089>
- Pozo-Vázquez, D., Tovar-Pescador, J., Gámiz-Fortis, S.R., Esteban-Parra, M.J. & Castro-Diez, Y. (2004) Nao and solar radiation variability in the european North Atlantic region. *Geophysical Research Letters*, 31(5). Available from: <https://doi.org/10.1029/2003gl018502>
- Santos-Alamillos, F.J., Pozo-Vázquez, D., Ruiz-Arias, J.A., Von Bremen, L. & Tovar-Pescador, J. (2015) Combining wind farms with concentrating solar plants to provide stable renewable power. *Renewable Energy*, 76, 539–550. Available from: <https://doi.org/10.1016/j.renene.2014.11.055>
- Schmidt, O., Melchior, S., Hawkes, A. & Staffell, I. (2019) Projecting the future levelized cost of electricity storage technologies. *Joule*, 3, 81–100. Available from: <https://doi.org/10.1016/j.joule.2018.12.008>
- Soret, A., Torralba, V., Cortesi, N., Christel, I., Palma, L.L., Manrique-Sunén, A. et al. (2019) *Sub-seasonal to seasonal climate predictions for wind energy forecasting*, Vol. 1222. Institute of Physics Publishing, Bilbao, Spain. Available from: <https://doi.org/10.1088/1742-6596/1222/1/012009>
- Tedesco, P., Lenkoski, A., Bloomfield, H.C. & Sillmann, J. (2022) Gaussian copula modeling of extreme cold and weak-wind

- events over Europe conditioned on winter weather regimes. *Environmental Research Letters*, 18, 034008.
- TSO. (2022) Szenariorahmen zum Netzentwicklungsplan Strom 2037 mit Ausblick 2045, Version 2023. Available at: [https://www.netzentwicklungsplan.de/sites/default/files/paragraphs-files/Szenariorahmenentwurf\\_NEP2037\\_2023.pdf](https://www.netzentwicklungsplan.de/sites/default/files/paragraphs-files/Szenariorahmenentwurf_NEP2037_2023.pdf). [Accessed 16th December 2022].
- van der Wiel, K., Stoop, L.P., van Zuijlen, B.R.H., Blackport, R., van den Broek, M.A. & Selten, F.M. (2019a) Meteorological conditions leading to extreme low variable renewable energy production and extreme high energy shortfall. *Renewable and Sustainable Energy Reviews*, 111, 261–275. Available from: <https://doi.org/10.1016/j.rser.2019.04.065>
- van der Wiel, K., Stoop, L.P., van Zuijlen, B.R.H., Blackport, R., van den Broek, M.A. & Selten, F.M. (2019b) The influence of weather regimes on European renewable energy production and demand. *Environmental Research Letters*, 14, 094010. Available from: <https://doi.org/10.1088/1748-9326/ab38d3>
- Vautard, R. (1990) Multiple weather regimes over the North Atlantic: analysis of precursors and successors. *Monthly Weather Review*, 118, 2056–2081. Available from: [https://doi.org/10.1175/1520-0493\(1990\)118%3C2056:MWROTN%3E2.0.CO;2](https://doi.org/10.1175/1520-0493(1990)118%3C2056:MWROTN%3E2.0.CO;2)
- Wernli, H. & Papritz, L. (2018) Role of polar anticyclones and mid-latitude cyclones for arctic summertime sea-ice melting. *Nature Geoscience*, 11, 108–113. Available from: <https://doi.org/10.1038/s41561-017-0041-0>
- White, C.J., Carlsen, H., Robertson, A.W., Klein, R.J.T., Lazo, J.K., Kumar, A. et al. (2017) Potential applications of subseasonal-to-seasonal (S2S) predictions. *Meteorological Applications*, 24, 315–325. Available from: <https://doi.org/10.1002/met.1654>
- White, C.J., Domeisen, D.I.V., Acharya, N., Adefisan, E.A., Anderson, M.L., Aura, S. et al. (2022) Advances in the application and utility of subseasonal-to-seasonal predictions. *Bulletin of the American Meteorological Society*, 103, E1448–E1472. Available from: <https://doi.org/10.1175/BAMS-D-20-0224.1>
- Zubiate, L., McDermott, F., Sweeney, C. & O'Malley, M. (2017) Spatial variability in winter NAO–wind speed relationships in western Europe linked to concomitant states of the East Atlantic and Scandinavian patterns. *Quarterly Journal of the Royal Meteorological Society*, 143(702), 552–562. Available from: <https://doi.org/10.1002/qj.2943>

## SUPPORTING INFORMATION

Additional supporting information can be found online in the Supporting Information section at the end of this article.

**How to cite this article:** Mockert, F., Grams, C. M., Brown, T., & Neumann, F. (2023). Meteorological conditions during periods of low wind speed and insolation in Germany: The role of weather regimes. *Meteorological Applications*, 30(4), e2141. <https://doi.org/10.1002/met.2141>